SAGE-Hindawi Access to Research
International Journal of Alzheimer's Disease
Volume 2011, Article ID 792070, 8 pages
doi:10.4061/2011/792070

Research Article

ApoE4-Driven Accumulation of Intraneuronal Oligomerized Aβ42 following Activation of the Amyloid Cascade *In Vivo* Is Mediated by a Gain of Function

Lia Zepa,[1] Moran Frenkel,[1] Haim Belinson,[1] Zehavit Kariv-Inbal,[1] Rakez Kayed,[2] Eliezer Masliah,[3] and Daniel M. Michaelson[1]

[1] *Department of Neurobiology, George S. Wise Faculty of Life Sciences, Tel Aviv University, Tel Aviv 69978, Israel*
[2] *George P. and Cynthia Woods Mitchell Center for Neurodegenerative Diseases, University of Texas Medical Branch, Galveston, TX 77555-0857, USA*
[3] *Departments of Neurosciences and Pathology, University of California San Diego, La Jolla, CA 92093-0624, USA*

Correspondence should be addressed to Daniel M. Michaelson, dmichael@post.tau.ac.il

Received 4 October 2010; Revised 21 November 2010; Accepted 3 December 2010

Academic Editor: Katsuhiko Yanagisawa

Activating the amyloid cascade by inhibiting the Aβ-degrading enzyme neprilysin in targeted replacement mice, which express either apoE4 or apoE3, results in the specific accumulation of oligomerized Aβ42 in hippocampal CA1 neurons of the apoE4 mice. We presently investigated the extent to which the apoE4-driven accumulation of Aβ42 and the resulting mitochondrial pathology are due to either gain or loss of function. This revealed that inhibition of neprilysin for one week triggers the accumulation of Aβ42 in hippocampal CA1 neurons of the apoE4 mice but not of either the corresponding apoE3 mice or apoE-deficient mice. At 10 days, Aβ42 also accumulated in the CA1 neurons of the apoE-deficient mice but not in those of the apoE3 mice. Mitochondrial pathology, which in the apoE4 mice is an early pathological consequence following inhibition of neprilyisn, also occurs in the apoE-deficient but not in the apoE3 mice and the magnitude of this effect correlates with the levels of accumulated Aβ42 and oligomerized Aβ42 in these mice. These findings suggest that the rate-limiting step in the pathological effects of apoE4 on CA1 neurons is the accumulation of intracellular oligomerized Aβ42 which is mediated via a gain of function property of apoE4.

1. Introduction

Apolipoprotein E (apoE) is a major brain lipoprotein and is expressed in humans as three common isoforms that differ from each other by one or two amino acids; these isoforms are termed apoE2 (Cys112, Cys158), apoE3 (Cys 112, Arg158), and apoE4 (Arg112, Arg158) [1, 2]. Genetic and epidemiological studies revealed that the allele ε4 of apoE is a strong genetic risk factor for early and late onset of Alzheimer's disease (AD) [3, 4]. More than 50% of AD patients carry the apoE ε4 allele which increases the risk for the disease by 2-3-fold in individuals who express one such allele and by more than 10-fold in subjects with two ε4 alleles [5, 6]. Histopathologically, apoE4 is associated in AD with increased amyloid deposition [7], and corresponding animal model and *in vitro* studies revealed synergistic pathological interactions between Aβ and apoE4 [4, 8–12] that are associated with cognitive deficits [13, 14]. This led to the suggestion that apoE4 potentiates the neurotoxic effects of Aβ and the amyloid cascade and drives them above a pathological threshold. The molecular mechanisms underlying the pathological cross-talk between Aβ and apoE and the extent to which they also mediate other pathological hallmarks of apoE4 in AD, such as impaired neuronal plasticity and repair [15–17] and increased brain inflammation [18], are currently not known. Another key unresolved issue is whether the pathological effects of apoE4 are due to the gain of a pathological property by apoE4 or to the loss of a protective function by this molecule, that the other apoE isoforms have.

We have recently shown that activation of the amyloid cascade by inhibiting the Aβ-degrading enzyme neprilysin

in targeted replacement mice that express either apoE4 or apoE3 results in the isoform-specific accumulation of Aβ42, oligomerized Aβ42, and apoE in CA1 neurons of the apoE4 mice, which in turn trigger mitochondrial pathology, neurodegeneration, and activation of cell death process [13, 19]. We presently investigate the extent to which the apoE4-driven intracellular accumulation and oligomerization of Aβ42 and the resulting mitochondrial impairments are due to either gain or loss of function of apoE4 relative to the AD benign isoform, apoE3. This was performed by inhibiting the Aβ-degrading enzyme neprilysin in apoE-deficient mice and in corresponding apoE4- and apoE3-targeted replacement mice. This was then followed by investigation of the resulting effects of apoE deficiency on the accumulation and oligomerization of Aβ42 and the associated neuropathology in CA1 neurons and of the extent to which they are similar to those observed in either the apoE4 or the apoE3 mice.

2. Materials and Methods

2.1. Transgenic Mice and Implantation of Alzet Miniosmotic Pumps. ApoE-targeted replacement mice (apoE mice), created by gene targeting [20], were purchased from Taconic. The mice were back-crossed to C57BL/6J mice for eight generations and were homozygous for either the apoE3 (3/3) or the apoE4 (4/4) allele. ApoE-deficient mice were purchased from Jackson Laboratories and were on the same background. The experiments were performed utilizing 4-month-old male apoE3, apoE4, and apoE-deficient mice whose genotypes were confirmed by PCR analysis [13, 21]. All experiments were approved by the Tel Aviv University Animal Care Committee, and every effort was made to minimize animal usage and reduce animal stress. Alzet miniosmotic pumps (model 2001, which deliver their contents at 0.25 μl/h for up to 14 days) were loaded with the neprilysin inhibitor thiorphan (0.5 mM; Sigma) in artificial cerebrospinal fluid containing 1 mM ascorbic acid or with a similar solution without thiorphan "sham." The Alzet pumps were implanted with a brain infusion canola inserted into the lateral ventricle as previously described [13].

2.2. Immunofluorescence and Confocal Microscopy. Thiorphan and sham-treated mice were anesthetized with ketamine xylazine at the indicated times following implantation of the Alzet pumps. The brains of these mice were then processed for immunoflourescence after which free-floating frozen coronal sections (30 μm) were treated with 70% formic acid for 7 min and then immunostained as previously described [13]. Aβ42 and oligomerized Aβ42 were detected utilizing rabbit anti-Aβ42 (dilution 1 : 500 from Chemicon) and biotinylated I-11 (dilution 1 : 2000) provided by Dr. Rakez Kayed, whereas the mitochondrial marker COX-1 was detected utilizing goat anti-COX-1 (1 : 400, from Santa Cruz Biotechnology). The bound primary antibodies were then visualized by incubating the sections with the appropriate fluorescently labeled second antibody, or with fluorescently labeled streptavidin as previously described [13]. The sections (between bregma -2.0 and -3.0) were visualized using a confocal scanning laser microscope (Zeiss, LSM 510). Images (1024 $\times$ 1024 pixels) were obtained by averaging eight scans per slice. Control experiments revealed no staining in stained sections lacking the first antibody. The intensities of immunofluorescence staining, expressed as the percentage of the area stained, were calculated utilizing the Image-Pro Plus system (version 5.1, Media Cybernetics) as previously described [13]. Two sections were analyzed per brain, and each staining was performed at least twice. All the images for each immunostaining were obtained under identical conditions, and their quantitative analyses were performed with no further handling. Moderate adjustments for contrast and brightness were performed on the images when the figures were prepared but were the same for the images of the different mouse groups. For the Aβ42 and I-11 and the COX-1 and Aβ42 double labeling colocalization experiments, each image was first analyzed separately to determine the percentage of the area stained and then to determine the percentage of the area of the two images that colocalize. Measurements of the contribution of stochastic processes to the co-localization data, which were performed by shifting the channels of one of the images laterally by 1 μm^2, revealed that the contribution of stochastic processes in all the experiments was negligible.

2.3. Immunoblot Analysis. Hippocampi were homogenized (20% w/v) in PBS, pH 7.4, with protease inhibitor cocktail (Roche, # 1 836 153) and centrifuged at 10,000 rpm for 5 min, after which the supernatant (PBS extract) was collected. The resulting pellet was extracted by resuspension in an equal volume of 10 mM Tris pH 7.6 containing 150 mM NaCl, 2 mM EDTA, protease inhibitor cocktail (Roche), and 1% NP-40, after which it was centrifuged for 5 min at 10,000 rpm and the resulting supernatant (NP-40 extract) was collected. SDS gel electrophoresis utilizing 12% SDS and immunoblotting with mAb 266 (Elan pharmaceuticals) were then performed as previously described [19]. Intensities of the immunoblot bands were quantified by using EZQuant-Gel software (EZQuant, Tel-Aviv, Israel).

2.4. Statistical Analysis. It was performed using SPSS version 14. The effects of treatment in the apoE-deficient mice (e.g., sham and thiorphan-treated mice) and in the thiorphan-treated apoE3-, apoE4-, and apoE-deficient mice at the 7-day time point were each analyzed by one-way ANOVA. In the 10-day experiment, in which both sham- and thiorphan-treated mice in all three mouse groups were investigated, the results were analyzed by two-way ANOVA. When appropriate, these results were further subjected to post hoc analysis by Student's t-test utilizing Bonferroni correction for multiple comparisons.

3. Results

Immunofluorescence measurements of the levels of Aβ42 in hippocampal CA1 neurons of apoE-deficient mice and their comparison to those of the corresponding apoE3 and apoE4 targeted replacement mice are depicted in Figure 1(a). As shown, the Aβ42 levels of the apoE deficient mice were not affected by the thiorphan treatment at day 7; they were

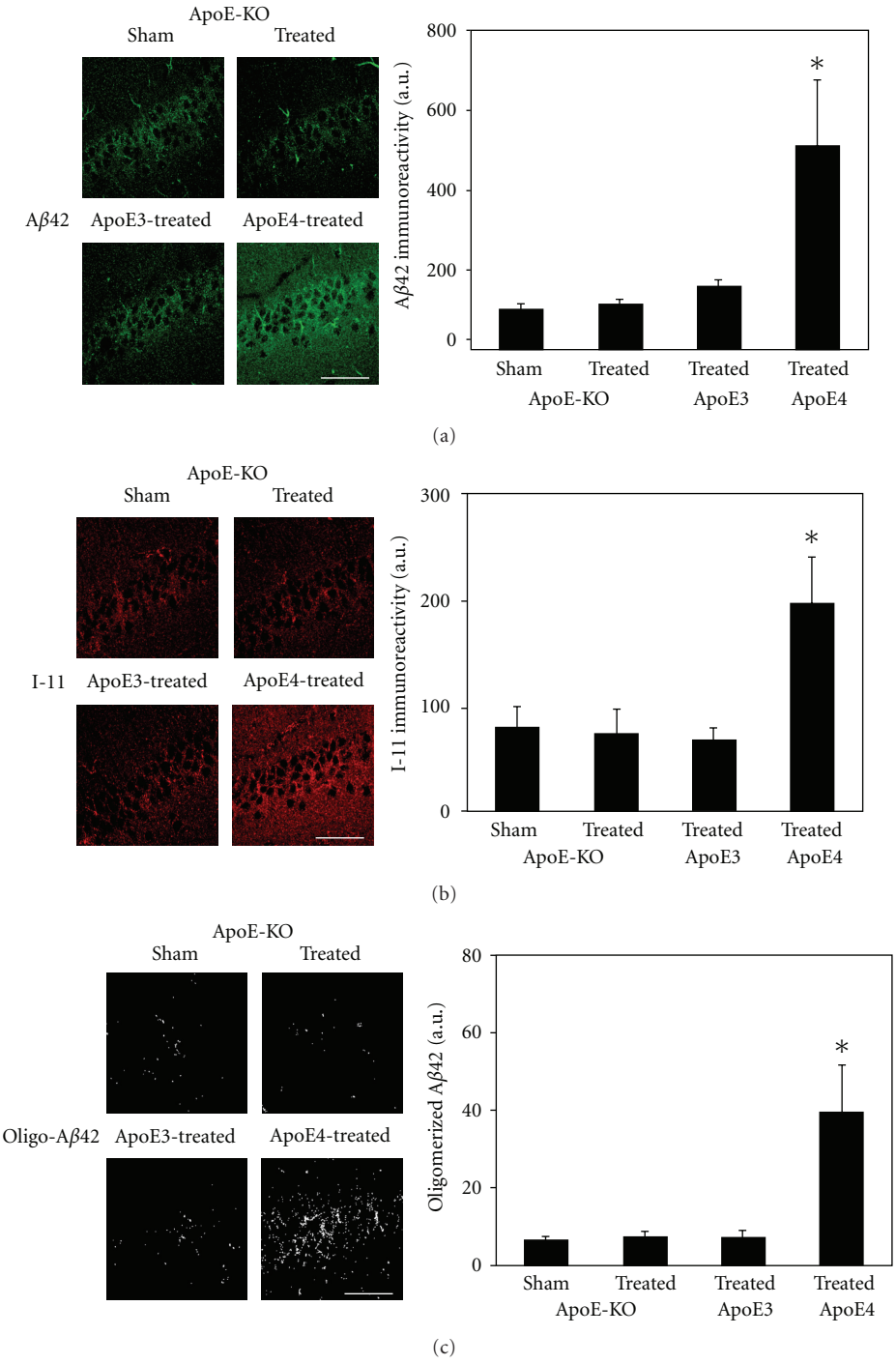

Figure 1: The effects of apoE3, apoE4, and apoE deficiency on the levels of Aβ42 and oligomerized Aβ42 in CA1 hippocampal neurons following inhibition of neprilysin. ApoE3, apoE4, and apoE-deficient male mice were injected i.c.v. with the neprilysin inhibitor thiorphan or sham-treated for 7 days, after which their brains were excised and subjected to anti-Aβ42 and anti-I-11 immunofluorescence, as described in "Materials and Methods." (a) Representative coronal sections of sham- and thiorphan-treated apoE-deficient mice (upper row) and thiorphan-treated apoE3 and apoE4 mice (lower row) immunostained with anti-Aβ42 are shown on the left (bar = 50 μm). Quantification of the density of Aβ42 staining (mean ± SEM; n = 5–6 mice/group in the sham- and thiorphan-treated groups) in the CA1 neurons of the indicated mice is shown on the right. $P < .05$ for the effects of treatment on the three mouse groups by one-way ANOVA. (b) Representative confocal images of I-11 of the CA1 area of the indicated mouse groups treated for 7 days with thiorphan (left) and quantification (right) of the density of I-11 staining (mean ± SEM; n = 5–6 mice/group in the sham- and thiorphan-treated groups) (mean ± SEM; n = 4–5). $P < .03$ for the effect of treatment on the three mouse groups by one-way ANOVA. (c) Representative masked oligo-Aβ42 images of the CA1 area of the indicated mouse groups treated for 7 days with thiorphan (left) and quantification (right) of the density of oligo-Aβ42 staining (mean ± SEM; n = 5–6 mice/group in the sham- and thiorphan-treated groups). $P < .05$ for the effect of treatment on the three mouse groups by one-way ANOVA.

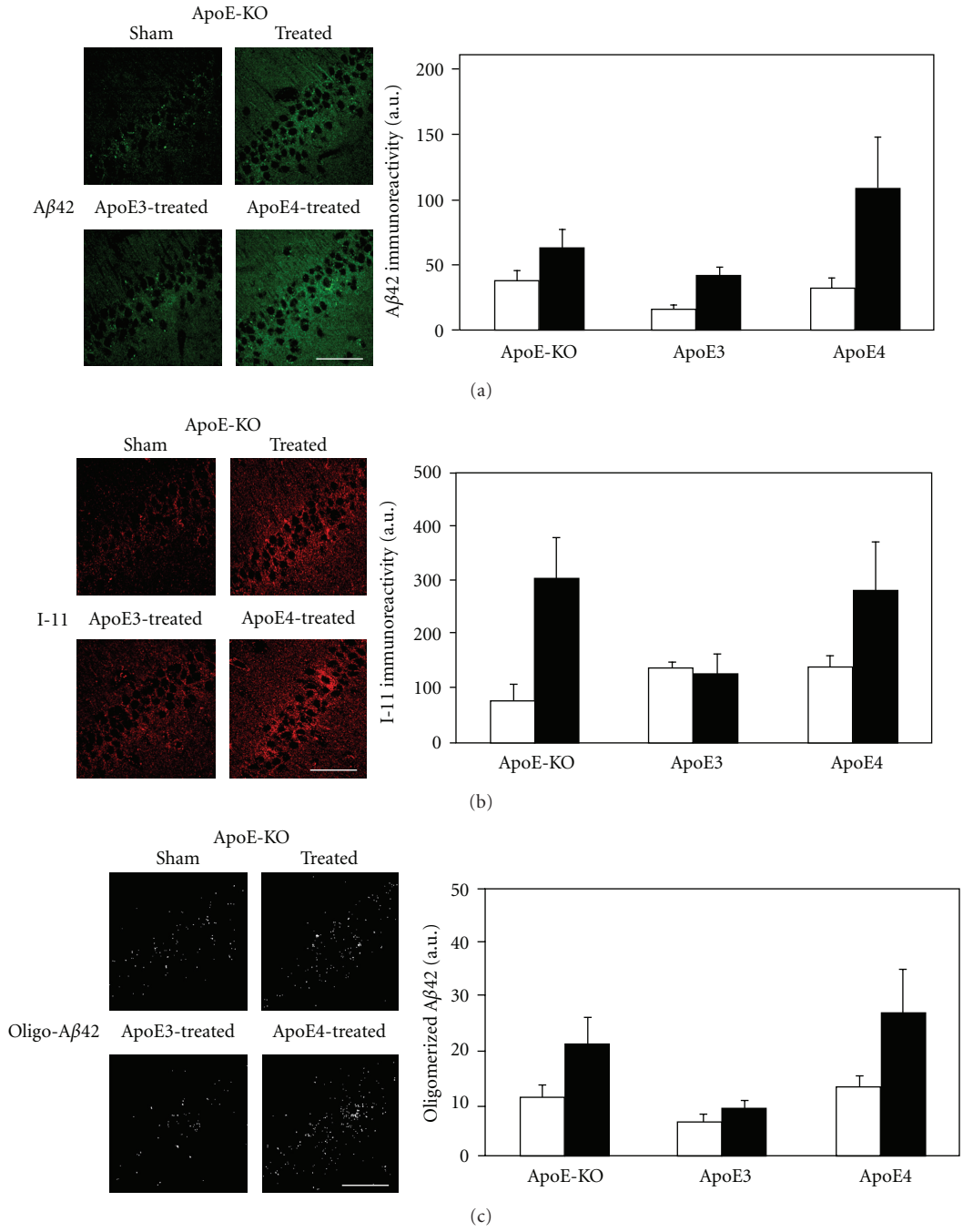

Figure 2: The effects of apoE3, apoE4, and apoE deficiency on the levels of Aβ42 and oligomerized Aβ42 in CA1 hippocampal neurons following inhibition of neprilysin. ApoE3-, apoE4- and apoE-deficient male mice were injected i.c.v. with the neprilysin inhibitor thiorphan; or sham-treated for 10 days, after which their brains were excised and subjected to anti-Aβ42 and anti-I-11 immunfluorescence, as described in "Materials and Methods." (a) Representative coronal sections of sham- and thiorphan-treated apoE-deficient mice (upper row) and thiorphan-treated apoE3 and apoE4 mice (lower row) immunostained with anti-Aβ42 are shown on the left (bar = 50 μm). Quantification of the density of Aβ42 staining (mean ± SEM; $n = 4$–5 mice/group) in the CA1 neurons of the indicated mice is shown on the right (empty and filled bars correspond, resp., to sham- and thiorphan-treated mice). $P < .02$ for the effects of treatment on the three mouse groups by two-way ANOVA. (b) Representative confocal images of I-11 of the CA1 area of the indicated mouse groups treated for 10 days with thiorphan (left) and quantification (right) of the density of I-11 staining (mean ± SEM; $n = 4$–5 mice/group). Empty and filled bars correspond, respectively, to sham- and thiorphan-treated mice and $P < .02$ for the effect of treatment by two-way ANOVA. (c) Representative masked oligo-Aβ42 images of the CA1 area of the indicated mouse groups treated for 10 days with thiorphan (left) and quantification (right) of the density of oligo-Aβ42 staining (mean ± SEM; $n = 4$–5 mice/group). Empty and filled bars correspond, respectively, to sham- and thiorphan-treated mice and $P < .02$ for the effect of treatment by two-way ANOVA.

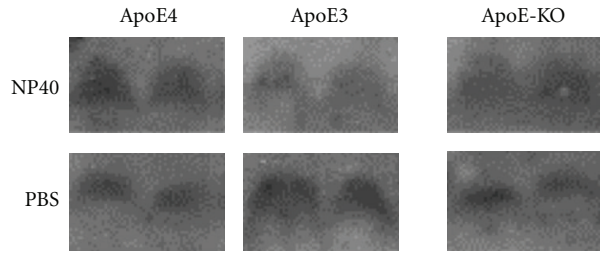

Figure 3: Aβ42 immunoblot of the hippocampal CA1 field of apoE4, apoE3, and apoE-deficient mice. The mice were treated for 10 days with thiorphan after which they were killed and their hippocampus was extracted and immunoblotted with the anti-Aβ42 Ab 266 as described in "Materials and Methods." Membrane bound NP40 extractable Aβ42 (apparent molecular weight 4.5 kD) is shown in the upper panels whereas the corresponding PBS extractable soluble Aβ42 is shown in the lower panels.

similar to those of the thiorphan-treated apoE3 mice and were significantly lower than those of the thiorphan-treated apoE4 mice ($P < .05$; Figure 1(a)). Further measurements of the effects of apoE on the accumulation of oligomerized Aβ42 were performed utilizing Ab I-11, which is directed specifically at the backbone of amyloid oligomers [22, 23]. This revealed that at day 7, and in accordance with the Aβ42 results, the thiorphan treatment induced I-11 immunoreactivity to accumulate in the CA1 neurons of the apoE4 but not in those of either the apoE3 mice or the apoE-deficient mice ($P < .03$; Figure 1(b)). The I-11 and Aβ42 immunoreactivities of the individual apoE4 mice were highly correlated ($R^2 = 0.9$). I-11 recognizes amyloid-like structures derived from Aβ as well as non-Aβ peptides [23]. Accordingly, the levels of I-11 in the different mouse groups that correspond to oligomerized Aβ42 were determined by double labeling confocal experiments utilizing I-11 and anti-Aβ42. This revealed significant co-localization of these stains and of their merged image, which we will term here "oligo-Aβ42," in the CA1 neurons of the apoE4 mice (Figure 1(c)). In contrast, and in agreement with the single labeling experiments, the levels of oligo-Aβ42 in CA1 neurons of the apoE-deficient and apoE3 mice were similar and low.

Additional measurements of the levels of Aβ42, I-11, and oligo-Aβ42 in the different mouse groups were also performed on day 10 after the thiorphan treatment began. This revealed that, unlike at the earlier time point, the levels of Aβ42, I-11, and oligo-Aβ42 of the apoE-deficient mice were now elevated and comparable to those observed with the apoE4 mice (Figure 2; $P < .02$ for the effect of treatment by 2-way ANOVA). Importantly, the corresponding levels of Aβ42, I-11, and oligo-Aβ42 in the apoE3 mice were not increased by the thiorphan treatment even at 10 days (Figure 2).

Previous immunoblot experiments utilizing hippocampal homogenates revealed that the thiorphan-treated apoE3 and apoE4 mice have similar Aβ42 levels but that in the apoE4 most of the Aβ42 is membrane-bound whereas in the apoE3 mice it is soluble [19]. Accordingly, we next investigated the extent to which apoE deficiency affects the levels and solubility of the accumulated Aβ42. As shown in Figure 3 the levels of the membrane-bound NP40 extractable Aβ42 and of the soluble PBS extractable Aβ42 pools of the apoE-deficient mice were intermediate to those of the apoE3 and apoE4 mice. Furthermore, the total levels of soluble and insoluble pools were similar in the apoE4, apoE deficient, and apoE3 mice (resp., 100 ± 30%, 91 ± 17% and 91 ± 18%). Comparison of these results to the immunoflourescence findings (compare Figures 2 and 3 both of which were obtained at day 10) revealed that the relative levels of the NP40 extractable Aβ42 pools and of the accumulation of intracellular Aβ42 in the different mice groups have the same rank order (apoE4 > apoE deficient > apoE3) suggesting that the accumulated intracellular Aβ42 is membrane bound.

We have recently shown by electron microscopy that the specific accumulation of Aβ42 in CA1 neurons of apoE4 mice following inhibition of neprilysin is associated with marked mitochondrial deformation and with the colocalization of Aβ in the affected mitochondria [19]. Complementary immunofluorescence confocal microscopy experiments revealed that the mitochondrial pathology is associated with increased levels of mitochondrial COX-1 immunoreactivity and with the colocalization of Aβ42 with COX-1 [19]. Utilizing COX-1 as a marker of mitochondrial pathology, we investigated the extent to which inhibition of neprilysin in the mice affects their mitochondria. This revealed that mitochondrial pathology at 7 days, like the accumulation of Aβ42 and oligo-Aβ42, occurs only in the apoE4 mice (not shown). In contrast, at day 10 it occurred in both the apoE4 and the apoE-deficient mice but not in the apoE3 mice (Figure 4(a)). Furthermore, the magnitude of the mitochondrial effect and the levels of Aβ42 in the apoE-deficient were both similarly lower in the apoE-deficient than the apoE4 mice (compare Figures 2 and 4). Co-localization confocal microscopy revealed that the Aβ42 which accumulates in CA1 neurons of the apoE-deficient mice, like that of the corresponding apoE4 mice [19], colocalizes with mitochondria (Figure 4(b)). The findings that the levels of mitochondrial pathology and of Aβ42 and oligomerized Aβ42 in the CA1 neurons of the different mice groups correlate suggest that the main and rate-limiting effect of apoE4 on the mitochondria is due to stimulation of the accumulation of Aβ42 and oligomerized Aβ42.

4. Discussion

The present study revealed that apoE4 triggers the accumulation of Aβ42 in hippocampal CA1 neurons during the early phase (i.e., 7 days), following activation of the amyloid cascade *in vivo* and that this effect is specific to apoE4 and does not occur in either apoE3 or apoE-deficient mice. This effect reflects differences in the extent of accumulation of Aβ42, since the total hippocampal Aβ42 contents, determined by immunoblots, were similarly elevated following inhibition of neprilysin in the ApoE3 and apoE4 mice [19] and in the apoE-deficient ones (not shown). The present findings are in accordance with previous *in vitro* cell culture studies [24–26] and suggest that the rate-limiting step in the apoE4-driven accumulation of Aβ42 is due to a gain of function.

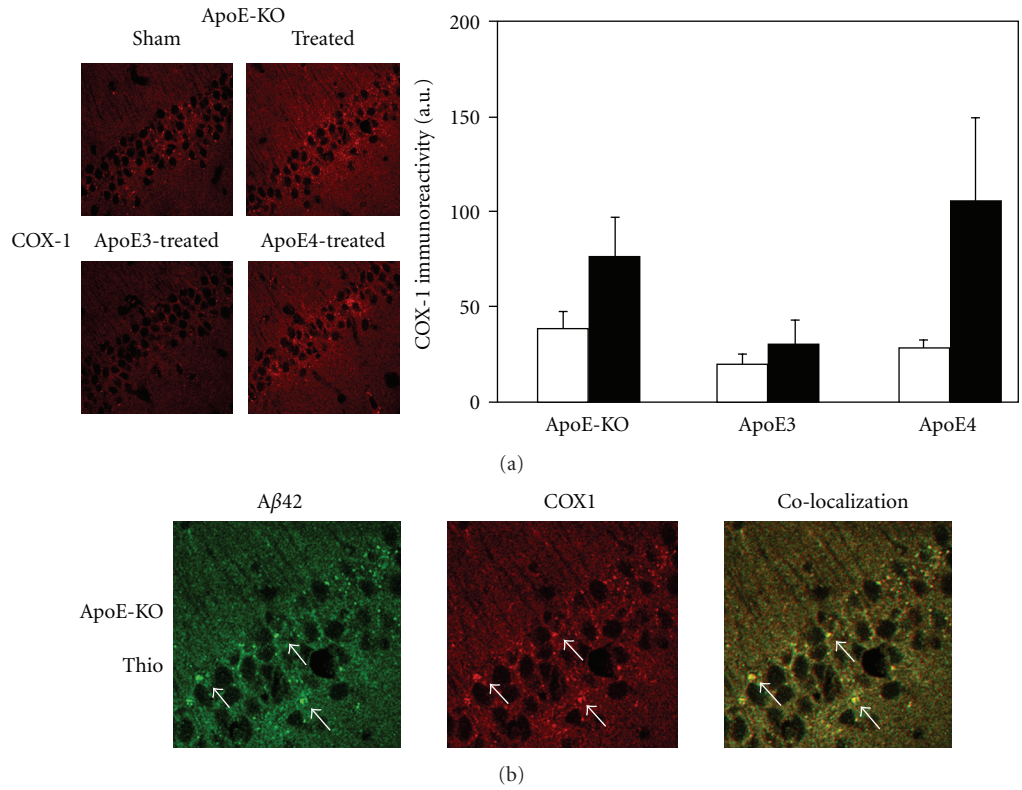

FIGURE 4: The effects of apoE3, apoE4, and apoE deficiency on the mitochondria of hippocampal CA1 neurons following inhibition of neprilysin. ApoE3, apoE4, and apoE-deficient male mice were injected i.c.v. with the neprilysin inhibitor thiorphan or sham-treated for 10 days, after which their brains were excised and subjected to COX-1 immunofluoresence as described in "Materials and Methods." (a) Representative coronal sections of sham- and thiorphan-treated apoE-deficient mice (upper row) and thiorphan-treated apoE3 and apoE4 mice (lower row) immunostained with anti-COX-1 are shown on the left (bar = 50 μm). Quantification of the density of staining (mean ± SEM; n = 4–5 mice/group in the sham- and thiorphan-treated groups) in the CA1 neurons of the indicated mice is shown on the right (empty and filled bars correspond, resp., to sham- and thiorphan-treated mice). $P < .03$ for the effects of treatment on the three mouse groups by Two-way ANOVA. (b) Representative confocal images of the co-localization of Aβ42 and COX-1 in the CA1 area of apoE-deficient mice treated with thiorphan for 10 days.

The finding that the I-11 immunoreactivity levels of the CA1 neurons in the apoE-deficient mice, like their Aβ42 levels, did not rise during the initial 7 days following the thiorphan treatment (Figure 1(b)) is in accordance with the observation that these molecules colocalize in the thiorphan-treated apoE4 mice (Figure 1(c)). Moreover, it suggests that thiorphan treatment in the apoE-deficient mice does not stimulate the production of non-Aβ amyloid molecules in the CA1 neurons.

At longer time intervals, following activation of the amyloid cascade by inhibition of neprilysin (i.e., 10 versus 7 days), this treatment also induces the accumulation of oligomerized Aβ42 in the CA1 neurons of the apoE-deficient mice but not those of the apoE3 mice (Figure 2). This may be a reflection of time-dependent differences in the apoE dependencies of the kinetics of Aβ42 accumulation, such that Aβ42 accumulation in the apoE-deficient mice is delayed relative to that observed with the apoE4 mice. Alternatively, since the extent of Aβ42 accumulation is determined by the interplay between uptake and clearance, it is also possible that apoE-related effects on the clearance of Aβ42 contribute significantly to the observed effects at 10 days. Indeed, it has recently been shown that the clearance of Aβ is more effective in apoE3 mice than in apoE4- and apoE-deficient mice [1, 27, 28]. This suggests that the observation that the levels of Aβ42 are particularly low in the thiorphan-treated apoE3 mice at 10 days (Figure 2(a)) may be due, at least in part, to enhanced clearance of Aβ42 by apoE3. Further studies are required for unraveling the role of clearance-related mechanisms in mediating the effects of the different apoE isoforms and of apoE deficiency on the intracellular levels of Aβ42.

Examination of the effects of apoE-deficiency on the oligomerization of Aβ42 revealed that whereas the levels of Aβ42 in the apoE-deficient mice at 10 days are lower than those of the apoE4 mice (Figure 2(a)), the two mice groups have similar levels of oligomerized Aβ42 (Figures 2(b) and 2(c)). This suggests that either apoE does not play a rate-limiting role in the early stages of oligomerization of Aβ42 which are detected with I-11, or that apoE deficiency has an indirect stimulatory effect on the aggregation of Aβ42.

The levels of Aβ42 and oligomerized Aβ42 in the CA1 neurons of the different mice groups and time points reveal that they correlate positively with the corresponding levels of mitochondrial pathology (Figures 1, 2, 4). This suggests that the limiting step in the observed effects of apoE4 on the mitochondria is stimulation of the accumulation and the oligomerization of Aβ42. One implication of this conclusion is that the effects of apoE4 on the mitochondria are not mediated via direct effects of apoE4 on the mitochondria, which is consistent with our recent finding that the apoE4 which accumulates in CA1 neurons following inhibition of neprilysin does not colocalize with mitochondria [19].

The mechanisms underlying the accumulation of Aβ42 and oligomerized Aβ42 in the mitochondria are not fully understood. Since Aβ42 also accumulates in the lysosome of the CA1 neurons of the neprilysin inhibited apoE4 mice [19], it is possible that Aβ42 reaches the cytoplasm and the mitochondria via the lysosomal pathway and lysosomal leakage. Alternately since extracellularly applied Aβ42 accumulates in the mitochondria of neuronal cultures [29], it is also possible that the extracelluar Aβ42 which accumulates following inhibition of neprilysin reaches the mitochondria via this route.

In conclusion, the present findings show that the isoform-specific accumulation of Aβ42 and oligomerized Aβ42 in hippocampal neurons, following activation of the amyloid cascade *in vivo,* is mediated by a gain-of-function property of apoE4. Furthermore, since the resulting mitochondrial pathology correlates with the levels of accumulated Aβ42 and oligomerized Aβ42, this suggests that the overall pathological effects of apoE4 in this system are driven by the effects of apoE4 on the accumulation of Aβ42 and that consequently an anti-apoE4 therapeutic strategy may be effective in counteracting the synergistic pathological effects of apoE4 and Aβ42.

Acknowledgments

The authors thank Mr. Ori Liraz for many helpful discussions and Elan Pharmaceutics for the gift of MAb 266. This work was supported in part by grants from the Israel Science Foundation and from the Joseph and Inez Eichenbaum Foundation, and by the LIPIDIDIET grant funded by the 7th Framework Program of the European Union. D. M. Michaelson is the incumbent of the Myriam Lebach Chair in Molecular Neurodegeneration.

References

[1] J. Kim, J. M. Basak, and D. M. Holtzman, "The role of apolipoprotein E in Alzheimer's disease," *Neuron*, vol. 63, no. 3, pp. 287–303, 2009.

[2] R. W. Mahley and S. C. Rall, "Apolipoprotein E: far more than a lipid transport protein," *Annual Review of Genomics and Human Genetics*, vol. 1, no. 2000, pp. 507–537, 2000.

[3] E. H. Corder, A. M. Saunders, W. J. Strittmatter et al., "Gene dose of apolipoprotein E type 4 allele and the risk of Alzheimer's disease in late onset families," *Science*, vol. 261, no. 5123, pp. 921–923, 1993.

[4] W. J. Strittmatter, K. H. Weisgraber, D. Y. Huang et al., "Binding of human apolipoprotein E to synthetic amyloid β peptide: isoform-specific effects and implications for late-onset Alzheimer disease," *Proceedings of the National Academy of Sciences of the United States of America*, vol. 90, no. 17, pp. 8098–8102, 1993.

[5] L. Bertram, M. B. McQueen, K. Mullin, D. Blacker, and R. E. Tanzi, "Systematic meta-analyses of Alzheimer disease genetic association studies: the AlzGene database," *Nature Genetics*, vol. 39, no. 1, pp. 17–23, 2007.

[6] B. T. Hyman, T. Gomez-Isla, G. W. Rebeck et al., "Epidemiological, clinical, and neuropathological study of apolipoprotein E genotype in Alzheimer's disease," *Annals of the New York Academy of Sciences*, vol. 802, pp. 1–5, 1996.

[7] D. E. Schmechel, A. M. Saunders, W. J. Strittmatter et al., "Increased amyloid β-peptide deposition in cerebral cortex as a consequence of apolipoprotein E genotype in late-onset Alzheimer disease," *Proceedings of the National Academy of Sciences of the United States of America*, vol. 90, no. 20, pp. 9649–9653, 1993.

[8] I. Dolev and D. M. Michaelson, "A nontransgenic mouse model shows inducible amyloid-β (Aβ) peptide deposition and elucidates the role of apolipoprotein E in the amyloid cascade," *Proceedings of the National Academy of Sciences of the United States of America*, vol. 101, no. 38, pp. 13909–13914, 2004.

[9] D. M. Holtzman, "In vivo effects of ApoE and clusterin on amyloid-beta metabolism and neuropathology," *Journal of Molecular Neuroscience*, vol. 23, no. 3, pp. 247–254, 2004.

[10] J. Jordán, M. F. Galindo, R. J. Miller, C. A. Reardon, G. S. Getz, and M. J. LaDu, "Isoform-specific effect of apolipoprotein E on cell survival and β-amyloid-induced toxicity in rat hippocampal pyramidal neuronal cultures," *Journal of Neuroscience*, vol. 18, no. 1, pp. 195–204, 1998.

[11] M. J. LaDu, M. T. Falduto, A. M. Manelli, C. A. Reardon, G. S. Getz, and D. E. Frail, "Isoform-specific binding of apolipoprotein E to β-amyloid," *Journal of Biological Chemistry*, vol. 269, no. 38, pp. 23403–23406, 1994.

[12] P. S. Puttfarcken, A. M. Manelli, M. T. Falduto, G. S. Getz, and M. J. LaDu, "Effect of apolipoprotein E on neurite outgrowth and β-amyloid-induced toxicity in developing rat primary hippocampal cultures," *Journal of Neurochemistry*, vol. 68, no. 2, pp. 760–769, 1997.

[13] H. Belinson, D. Lev, E. Masliah, and D. M. Michaelson, "Activation of the amyloid cascade in apolipoprotein E4 transgenic mice induces lysosomal activation and neurodegeneration resulting in marked cognitive deficits," *Journal of Neuroscience*, vol. 28, no. 18, pp. 4690–4701, 2008.

[14] P. van Meer, S. Acevedo, and J. Raber, "Impairments in spatial memory retention of GFAP-apoE4 female mice," *Behavioural Brain Research*, vol. 176, no. 2, pp. 372–375, 2007.

[15] T. Arendt, C. Schindler, M. K. Brückner et al., "Plastic neuronal remodeling is impaired in patients with Alzheimer's disease carrying apolipoprotein ε4 allele," *Journal of Neuroscience*, vol. 17, no. 2, pp. 516–529, 1997.

[16] B. Teter, "ApoE-dependent plasticity in Alzheimer's disease," *Journal of Molecular Neuroscience*, vol. 23, no. 3, pp. 167–179, 2004.

[17] F. White, J. A. R. Nicoll, A. D. Roses, and K. Horsburgh, "Impaired neuronal plasticity in transgenic mice expressing human apolipoprotein E4 compared to E3 in a model of entorhinal cortex lesion," *Neurobiology of Disease*, vol. 8, no. 4, pp. 611–625, 2001.

[18] R. Egensperger, S. Kösel, U. von Eitzen, and M. B. Graeber, "Microglial activation in Alzheimer disease: association with APOE genotype," *Brain Pathology*, vol. 8, no. 3, pp. 439–447, 1998.

[19] H. Belinson, Z. Kariv-Inbal, R. Kayed, E. Masliah, and D. M. Michaelson, "Following activation of the amyloid cascade, apolipoprotein E4 drives the in vivo oligomerization of amyloidβ resulting in neurodegeneration," *Journal of Alzheimer's Disease*, vol. 22, no. 3, pp. 959–970, 2010.

[20] P. M. Sullivan, H. Mezdour, Y. Aratani et al., "Targeted replacement of the mouse apolipoprotein E gene with the common human APOE3 allele enhances diet-induced hypercholesterolemia and atherosclerosis," *Journal of Biological Chemistry*, vol. 272, no. 29, pp. 17972–17980, 1997.

[21] O. Levi, A. L. Jongen-Relo, J. Feldon, A. D. Roses, and D. M. Michaelson, "ApoE4 impairs hippocampal plasticity isoform-specifically and blocks the environmental stimulation of synaptogenesis and memory," *Neurobiology of Disease*, vol. 13, no. 3, pp. 273–282, 2003.

[22] R. Kayed and C. G. Glabe, "Conformation-Dependent Anti-Amyloid Oligomer Antibodies," *Methods in Enzymology*, vol. 413, pp. 326–344, 2006.

[23] R. Kayed, E. Head, J. L. Thompson et al., "Common structure of soluble amyloid oligomers implies common mechanism of pathogenesis," *Science*, vol. 300, no. 5618, pp. 486–489, 2003.

[24] U. Beffert, N. Aumont, D. Dea, S. Lussier-Cacan, J. Davignon, and J. Poirier, "β-amyloid peptides increase the binding and internalization of apolipoprotein E to hippocampal neurons," *Journal of Neurochemistry*, vol. 70, no. 4, pp. 1458–1466, 1998.

[25] U. Beffert, N. Aumont, D. Dea, S. Lussier-Cacan, J. Davignon, and J. Poirier, "Apolipoprotein E isoform-specific reduction of extracellular amyloid in neuronal cultures," *Molecular Brain Research*, vol. 68, no. 1-2, pp. 181–185, 1999.

[26] K. Yamauchi, M. Tozuka, H. Hidaka, T. Nakabayashi, M. Sugano, and T. Katsuyama, "Isoform-specific effect of apolipoprotein E on endocytosis of β-amyloid in cultures of neuroblastoma cells," *Annals of Clinical and Laboratory Science*, vol. 32, no. 1, pp. 65–74, 2002.

[27] M. J. Sharman, M. Morici, E. Hone et al., "APOE genotype results in differential effects on the peripheral clearance of amyloid-β42 in APOE knock-in and knock-out mice," *Journal of Alzheimer's Disease*, vol. 21, no. 2, pp. 403–409, 2010.

[28] R. Deane, A. Sagare, K. Hamm et al., "ApoE isoform-specific disruption of amyloid β peptide clearance from mouse brain," *Journal of Clinical Investigation*, vol. 118, no. 12, pp. 4002–4013, 2008.

[29] C. A. H. Petersen, N. Alikhani, H. Behbahani et al., "The amyloid β-peptide is imported into mitochondria via the TOM import machinery and localized to mitochondrial cristae," *Proceedings of the National Academy of Sciences of the United States of America*, vol. 105, no. 35, pp. 13145–13150, 2008.